Nonmonotonic Scission and Branching Free Energies as Functions of Hydrotrope Concentration for Charged Micelles

Taraknath Mandal,[1,*] Peter H. Koenig,[2] and Ronald G. Larson[1,†]
[1]Department of Chemical Engineering, University of Michigan, Ann Arbor, Michigan 48109, USA
[2]Computational Chemistry, Modeling and Simulation, The Procter & Gamble Company, 8611 Beckett Road, West Chester, Ohio 45069, USA

(Received 11 November 2017; revised manuscript received 30 April 2018; published 16 July 2018)

Using coarse-grained molecular dynamics simulations and an umbrella sampling method that uses local surfactant density as a reaction coordinate, we directly calculate, for the first time, both the scission and branching free energies of a model charged micelle [cationic cetyltrimethylammonium chloride (CTAC)] in the presence of inorganic and organic salts (hydrotropes). We find that while inorganic salt only weakly affects the micelle scission energy, organic hydrotropes produce a strong, nonmonotonic dependence of both scission energy and branching on salt concentration. The nonmonotonicity in scission energy is traced to a competition between electrostatic screening of the repulsions among the surfactant head groups and thinning of the micellar core, which result from attachment of the hydrotropes to the micelle surface. We are able to correlate the nonmonotonicity in the scission energy of CTAC micelles with the peak observed experimentally in viscosity versus hydrotrope concentration and the location of this peak in CTAC solutions.

DOI: 10.1103/PhysRevLett.121.038001

The self-assembly of neutral or charged surfactant molecules in aqueous solution is regulated by inorganic salt or organic hydrotropes (i.e., organic ions), leading to diverse structures such as spheres; rods; and long wormlike, looped, and branched micelles [1–4]. The richness of micellar solution morphologies leads to numerous applications of surfactants in personal care products, oil-production fluids, and medicines and as drag-reduction agents for fluid transportation, among others [5–8]. Their effectiveness in these applications often depends on their rheological properties, which strongly depend on the size and structure of the micelles. Unlike polymers, micelles can merge to form longer micelles or branched micelles or they can break into smaller micelles, maintaining a dynamical equilibrium in solution. Their breakage and rejoining, and hence their size distribution and conformation, are determined by their scission and branching (free) energies. Cates and co-workers proposed a mean-field scaling law that the average length of a micelle should depend on scission energy E_{sciss} as $\bar{L} \sim \phi^{0.5} \exp(E_{\mathrm{sciss}}/2k_BT)$ [9] (this formula may not be valid at very low surfactant concentration as shown by Carl *et al.* [10]). Later, MacKintosh *et al.* suggested that E_{sciss} in Cates' theory should be replaced by a "reduced scission energy" E^e_{sciss} in the case of a charged micelle as repulsions amongst the charged surfactant heads reduce the effective scission energy [11,12]. However, experimental verification of this theory is difficult as the scission energy of the micelles is estimated only indirectly, i.e., from their average length, which is challenging to measure accurately even when they can be observed by cryo-TEM [3].

Thus, the average length of the micelles is usually measured indirectly through their rheology. Specifically, the ratio of the loss modulus at its local minimum (G''_{min}) with respect to frequency to the plateau modulus (G_p) is theoretically related to the average micelle length ($\bar{L}$), as $G''_{\mathrm{min}}/G_p \sim (L_e/\bar{L})^n$, where L_e is the average contour length between two successive entanglement points along the micelle and the exponent in the original derivation $n = 1$ [13] was found in refined calculations to be $n = 0.8$ [14]. Measuring G''_{min}/G_p at different temperatures and obtaining $L_e/\bar{L}$ as a function of temperature, the scission energy (E_{sciss}) can be obtained through the relationship $\bar{L} \sim \phi^{0.5} \exp(E_{\mathrm{sciss}}/2k_BT)$, if one can take L_e to be temperature independent [15–18], which, however, has been claimed to be incorrect [13]. In addition, the formula $G''_{\mathrm{min}}/G_p \sim L_e/\bar{L}$ is a highly approximate formula, which ignores the effects of high-frequency bending modes on the rheology, for example, and is expected to underpredict $\bar{L}$ [13,19,20]. Moreover, neither this nor any other method has yet been proposed that can estimate the branching free energy of the micelles. Although the self-assembly, dynamics, and rheology of micelles have been heavily studied both experimentally and computationally [19–26], a method for direct estimation of both micelle scission and branching (free) energy is lacking so far.

Here, we introduce a method to obtain by coarse-grained molecular dynamics simulations the effect of hydrotropes and inorganic salts on the breakage and branching free energies of micelles and apply this method to cationic cetyltrimethylammonium chloride (CTAC) micelles. To do

so, we follow the recent work of Koenig *et al.* [27] and use umbrella sampling simulations with a reaction coordinate that controls the preferred number of molecules within a scission region. We show that this reaction coordinate can be traversed reversibly, thereby demonstrating sufficient sampling of configurations to yield the thermodynamic free energy. We show that the nonmonotonic dependence of the simulated scission energy on hydrotrope concentration can be expressed as a sum of a positive contribution that is linear in the number of surfactant molecules per unit length of the micelle and a negative term that is quadratic in the micelle charge, as can be rationalized by simple physical considerations. Furthermore, we also compute the branching free energy of CTAC micelles as a function of hydrotrope concentration and use this and the scission free energy to explain the origin of the ubiquitous large peak in the viscosity of this micellar solution with increasing hydrotrope concentration.

All coarse-grained simulations were performed using the MARTINI [28] force field, which has been used extensively [4,23–25,29,30] to model these surfactant systems and has been shown to reproduce many experimental observations including the sphere-to-rod transition and shear-induced micelle stretching energy. Details of the simulation protocol are given in the Supplemental Material [31], which includes Refs. [32–36]. The scission energy of the micelle was computed using an umbrella sampling method in which the number of beads in the prechosen "scission region" was taken as the reaction coordinate. A harmonic potential $V(N) = \frac{1}{2}K(N - N_0)^2$ was applied to constrain the number of beads N in this region to a target value of N_0 in a given window. Here, N is the instantaneous value of the number of surfactant beads in the scission region and K is the spring constant of the harmonic potential. The dimensions of the scission region along the X and Y directions (perpendicular to the micelle axis) are the dimensions of the simulation box in these directions, and the width of the scission region along the Z direction is given by d, shown in Fig. 1. The initial configurations for each window were generated using steered MD simulations in which the number of beads in the scission region was decreased from 350 to 0 in steps of 5, thus creating a total of 71 windows. These configurations were then used for umbrella sampling simulations. Each window was equilibrated for 200 ns prior to a 50-ns-long production run. The Weighted Histogram Analysis Method was used to extract the potential of mean force (PMF) from the biased simulations. All umbrella sampling simulations were performed using the GROMACS [37] package patched with the PLUMED 2.2 software [38].

The PMF for breaking a linear micelle as a function of the number of surfactant beads in the scission region of width 3 nm ($d = 3$ nm) is shown in Fig. 2(a) for the CTAC micelle in the absence of any organic salt, but with an

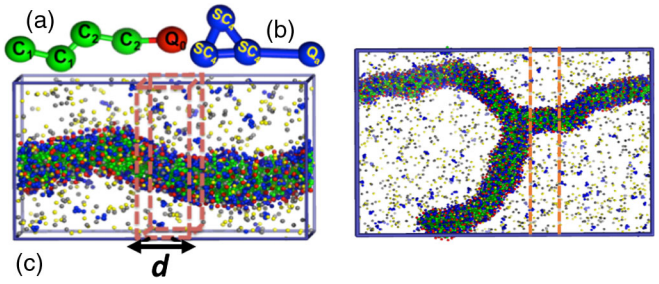

FIG. 1. Left panel: coarse-grained structure of (a) cationic CTA surfactant and (b) salicylate hydrotrope. Each bead is labeled with the MARTINI bead type. (c) Snapshot of the linear micelle in the presence of chloride counterions and NaSal hydrotropes. The dashed lines show the scission region where the biasing potential is applied. The arrow shows the width d of the scission region along the micelle axis. Right panel: Snapshot of the branched micelle. The dashed lines show the region where the biasing potential is applied. The green, red, blue, yellow, and gray beads represent the surfactant tail beads, surfactant head, salicylate, sodium, and chloride, respectively.

appropriate number of chloride ions to maintain charge neutrality. Starting from N close to 350, by applying a biasing potential, the numbers of beads in the scission region is driven down and the PMF rises to around 13.8 k_BT as shown in Fig. 2(a), corresponding to the beginning of a plateau in the PMF at around $N = 140$. The beginning of the plateau region corresponds to the breakage of the micelle, and the plateau region corresponds to the equilibrium state with two end caps; the beads in these end caps remain in the scission region until the micelle fragments are driven apart and the bead count drops towards zero. The PMF has a minimum at $N = 270$ beads in the scission region, which is the average number of surfactant beads per

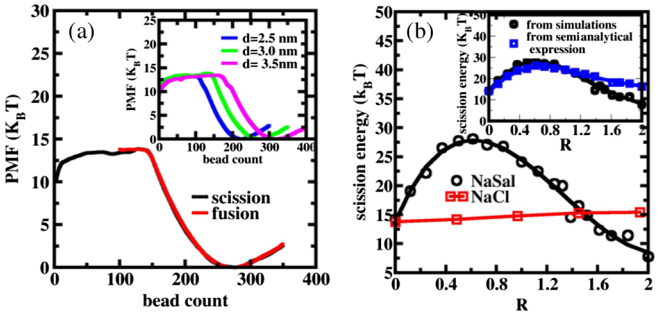

FIG. 2. (a) PMF as a function of the number of surfactant beads in the scission region in the absence of added salt. Inset shows the PMF for different widths (d) of the scission region. Error bars are of the order of the line width and hence are not shown. (b) Scission energy of the CTAC micelles as a function of R. The solid black line is a polynomial fit to the numerical data (circles). Error bars are of the order of the symbol size and hence are not shown. The inset compares the scission energy obtained from the simulations and a semianalytical expression discussed in the text.

3 nm of an equilibrated CTAC micelle. The free energy difference between the minimum and the plateau is the breakage free energy or "scission energy" of the micelles. The system contains two end caps after the breakage; hence, the end-cap free energy is half of the scission energy, which is $\sim 6.9 k_B T$. We also verified that the PMF is reversible [the red line Fig. 2(a)] with respect to the reaction coordinate and is independent of the width of the scission region d as shown in the Fig. 2(a) inset (see the Supplemental Material [31] for details).

We now discuss the effect of the inorganic salt NaCl and organic salt NaSal on the scission energy of the CTAC micelles. As shown in Fig. 2(b), the scission energy as a function of R, the ratio of the number of salt ion pairs to surfactant molecules, slightly increases with the NaCl concentration while the effect of the NaSal salt is much more prominent as we shall discuss later. The end-cap energy of a CTAC micelle in an NaCl solution at $R = 1$ is $\sim 7.5 k_B T$, which is roughly comparable to the end-cap energy of $\sim 10.6 k_B T$ for a CTAB micelle in a $NaNO_3$ solution at $R = 1$, as reported in a recent experimental study [39]. The modest difference in the scission energies is probably due to different inorganic salts (NaCl vs $NaNO_3$) considered in these two studies. In our simulations, the end-cap energy increases only by $\sim 0.4 k_B T$ as the salt concentration is increased from $R = 1$ to $R = 2$, which is not very significant. This small change is also consistent with the experimental result showing an increase of the end-cap energy by $\sim 0.7 k_B T$ for the CTAB/$NaNO_3$ system for a similar change in the salt concentration [39].

The effect of organic salt or hydrotrope NaSal on the scission energy of CTAC is much greater than the effect of the NaCl salt. As can be seen from Fig. 2(b), the scission free energy initially increases with the NaSal concentration until R reaches a critical value of ~ 0.65, beyond which the scission energy of the micelle decreases. The nonmonotonic dependence of the scission energy of the CTAC micelles (cationic) on the NaSal concentration obtained from our simulations can be understood qualitatively from a theory analogous to the theory of "reduced effective scission energy" $E^e_{\rm sciss} = E_{\rm sciss} - (l_B r v^{*2}/\phi^{0.5})$ originally proposed by MacKintosh *et al.* [11,12]. Here, l_B, r, v^*, and $E_{\rm sciss}$ are, respectively, the Bjerrum length, the radius of the micelle, the number of effective elementary charges per unit length of the charged micelle, and the scission energy of an uncharged micelle of radius r that has been neutralized by condensation of opposite ions onto the micelle surface (see the Supplemental Material [31] for more details). The formula of MacKintosh *et al.* is valid for micelles whose charge per unit length is very small and hence is not applicable to CTAC micelles for which the charge density is determined by strongly adsorbing hydrotropes rather than by the Bjerrum length. We propose that the effective scission energy can be expressed as $E^e_{\rm sciss}(n, Q) = An - BQ^2$. Here A and B are constants and n and Q are the number of surfactant molecules per unit micelle length and the total charge (micelle + adsorbed hydrotropes) per unit micelle length, respectively. The first term (An) is the contribution from the micelle cross sectional area $\pi r^2 \sim n/\rho$, where r is the micelle radius and ρ is the density of surfactant beads in the micelle (taken here to be constant); i.e., a thicker micelle has a higher scission energy. The second term (BQ^2) represents the decrease in scission energy because of the electrostatic repulsion amongst the charged surfactants (see the Supplemental Material [31] for more details). In the presence of only counterions and no added hydrotrope, Q is high, which reduces the effective scission energy. However, Q decreases with increasing hydrotrope concentration since salicylate ions are strongly adsorbed onto the micelle surface because of their strong affinity to the CTAC micelle, as reported in earlier studies [16,40,41]. Strong adsorption or penetration of the salicylate ions into the micelle outer surface causes elongation of the micelle along the axial direction and shrinkage in the radial direction. Figure 3(a), upper panel, shows the number of surfactant beads per 3 nm of the micelle length as a function of the NaSal concentration, which is obtained from the bead count at the minimum of the PMF [Fig. 2(a)]. The number of surfactant beads per unit length, which depends quadratically on the effective micelle radius (see the Supplemental Material [31] for more details), gradually decreases with the increasing hydrotrope concentration, and this decreases the scission energy. The effective scission energy initially increases with hydrotrope concentration since n does not decrease significantly [Fig. 3(a)], but Q^2 decreases significantly with hydrotrope concentration and $E^e_{\rm sciss}(n, Q)$ reaches a maximum at an optimum value of $R \sim 0.65$. Note that we might expect a maximum of $E^e_{\rm sciss}(n, Q)$ at $R \sim 1.02$ since $Q = 0$ at this hydrotrope concentration, if $E_{\rm sciss}(n, Q)$ were independent of the micelle radius r. However, at higher hydrotrope concentration ($R > 0.65$),

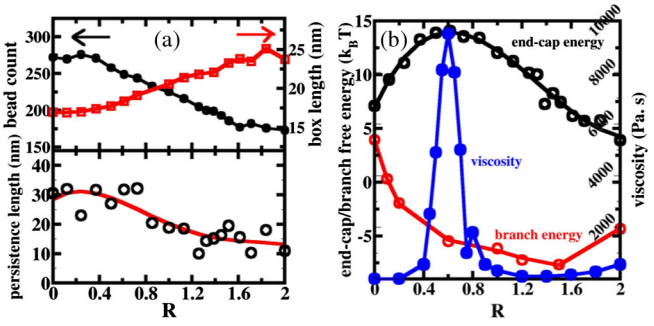

FIG. 3. (a) Average number of beads per 3 nm length of micelle and average box length along the micelle axis (upper panel) as well as persistence length of the CTAC micelle as a function of R (lower panel). The red line in the lower panel is a polynomial fit to the numerical data (circles). (b) End-cap free energy, branching free energy, and viscosity as functions of R for NaSal. Viscosity data are taken from Ref. [42].

n and r decrease significantly because of the micelle thinning and hence $E^e_{\rm sciss}(n,Q)$ starts to decrease before R reaches unity. At a still higher hydrotrope concentration, Q^2 eventually increases again as Q ultimately passes through zero at $R \sim 1.02$ and starts to increase in magnitude as the salicylate ions continue to be adsorbed onto the micelle surface and eventually penetrate into the interior of the micelle as reported earlier [16,40,41]. So, at $R > 1$, not only does n continue to decrease with increasing R, but also Q^2 begins to increase again, and hence $E^e_{\rm sciss}(n,Q)$ keeps decreasing when $R > 1.0$. Thus, at low R, micelle thinning (lower n) and cancellation of the micelle charge by adsorbed hydrotropes compete in their effects on scission energy, causing a maximum in $E^e_{\rm sciss}(n,Q)$ at $R < 1$, while at $R > 1$, both micelle thinning and the increase of the magnitude of the effective micelle charge by adsorbed hydrotropes act to decrease the scission energy. The simulated scission energy qualitatively follows the expression $E^e_{\rm sciss}(n,Q) = An - BQ^2$ as shown in the inset of Fig. 2(b). Details of the calculations are given in the Supplemental Material [31]. We do not expect, or observe, exact agreement with this simple formula for scission energy, since the mass density of surfactant within the micelle is not likely to be completely constant. We also note that beyond $R = 0.65$, the flexibility of the micelle increases (Fig. S2 [31]) and the persistence length decreases [Fig. 3(a)], which also make the micelle easier to break within this region. Note that the chloride ions of NaCl have much less affinity for the micelle surface than do the salicylate ions, as can be seen in Fig. S3 [31]. Most of the chloride ions remain in the solution while the salicylate ions concentrate at the micelle surface. As a result, Q and hence the effective scission energy are not affected as much by the NaCl salt as they are by NaSal.

Next, to compute the branching free energy, we decreased the bead count in the scission region of a branched micelle in such a way that an extra end cap was produced when the micelle body-branch bond was broken (Figs. S4 and S5 in Supplemental Material [31]). The micelle "body-branch bond energy" $[E_{\rm bond}(n,Q)]$ was computed using a similar umbrella sampling method as was used in the scission energy calculations. The reversibility of the process was also verified, as shown in Fig. S5 [31]. Note that when a micelle body-branch bond is broken, a branch point is lost and an end cap is gained. Thus, $E_{\rm bond}(n,Q) = [E^e_{\rm sciss}(n,Q)/2] - E_{\rm branch}(n,Q)$, where $E_{\rm branch}(n,Q)$ is the branching free energy of the micelle, which can be obtained from $E_{\rm bond}(n,Q)$ since $E^e_{\rm sciss}(n,Q)$ has been computed. Fig. 3(b) shows the branching free energy of the CTAC micelles as a function R in the presence of NaSal hydrotropes. At low values of R, the branching free energy is positive, suggesting that branch formation is unfavorable, which is consistent with a previous study [4]. However, the branching free energy decreases with R, implying that branch formation becomes more favorable at higher hydrotrope concentration, which is also consistent with previous studies [4]. To confirm further, we carried out self-assembly simulations by randomly dispersing surfactants in the simulation box at different hydrotrope concentrations. From this starting state, we observed spontaneous branch formation at all hydrotrope concentrations for which the branching free energies are negative (Fig. S7 [31]). Note that the branching free energy is positive even at $R = 2$ for NaCl (Fig. S5 [31]), suggesting that little branch formation should happen in the presence of NaCl only, which we also verified by simulation of self-assembly (Fig. S8 [31]) and which is also consistent with a previous study [4]. Interestingly, for NaSal, branching free energy is, like scission free energy, nonmonotonic, but with a minimum at $R = 1.5$, which is due to the competition between the micelle body-branch bond energy and the end-cap energy.

Since the viscosity should increase with the average length of the micelle, an increase in the scission energy with R at low R, with a maximum at $R = 0.65$ [Fig. 3(b)], is consistent with the experimental observation [42,43] of a rapid growth of the zero-shear viscosity of a CTAC micellar solutions with R up to around $R \sim 0.65$, followed by a decrease in viscosity thereafter [42]. It has been debated in the literature whether the decrease in the viscosity after this peak is due to branch points, whose sliding motion across the micelle body decreases the viscosity, or to a decrease in the mean length of the micelles [44–47]. Our results indicate that the latter explanation is more probable, since our computed scission energy significantly decreases for $R > 0.65$, while the branching energy shows a much weaker variation. Since branching should exist also for $0.15 < R < 0.65$, branch sliding may reduce the viscosity somewhat in this region, but according to our finding that the maximum in scission energy coincides with the viscosity maximum, the main contribution to the viscosity reduction apparently comes from the reduction in the average micelle length. This agrees with conclusions drawn in a previous experimental study [46,47]. Note that there should be significant branch and micelle network formation for $0.15 < R < 0.65$ as well as at higher R, due to negative branching free energy over the entire region $R > 0.15$. Thus, if the decrease in viscosity were due to branch formation, we would expect the first viscosity minimum to occur for a hydrotrope concentration $R < 0.65$. While the negative branch free energy, even below $R = 0.65$, implies the existence of micellar networks, these networks fragment and reorganize themselves more quickly when the end-cap energy is lower, and thus a maximum in viscosity occurs at $R = 0.65$ when the scission energy reaches a maximum. Significant branch formation before the first viscosity peak and a decrease in the average length of the micelles after the first viscosity peak have also been directly observed in a cryo-TEM study [47]. The weak effect of inorganic salt on the scission energy observed in our study

is also consistent with the experimental results of Khatory *et al.* [48] who showed that the viscosity of a CTAB/KBr solution increases by only eightfold upon a large increase of salt concentration from $R = 1.1$ to $R = 5.7$, while for CTAC/NaSal, the increase is 5 orders of magnitude over a smaller range of R [42]. Finally, we also note that Oelschlaeger *et al.* [15] estimated the scission energy of CPyCl/NaSal solutions as a function of R using the indirect method involving the plateau and loss moduli described above and found that the dependence of scission energy on R mimics the dependence of viscosity on R; i.e., it contains two peaks. However, our direct simulations of CTAC/NaSal show a single peak for the scission energy. In their calculation of scission free energy from the temperature-dependent rheological data, Oelschlaeger *et al.* [15] assumed the entanglement spacing L_e to be temperature independent, whereas it actually has a dependence of $L_e \propto T^{0.55}$ [13]. Moreover, they assumed that the growth law follows Cates' theory for linear micelles $G''_{\min}/G_p \sim L_e/\bar{L} \sim \exp(-E_{\text{sciss}}/2k_BT)$ even at high R where branches and networks are likely to form [4]. Therefore, the estimation of E_{sciss} from this method may be only approximate, especially if loops and networks are present.

In summary, we have described a method for calculating scission and branching free energy for micelles using molecular dynamics simulations combined with a weighted histogram method. Both scission and branching free energy for the CTAC micelle obtained from our simulations are nonmonotonic functions of hydrotrope concentration; the former shows a maximum at $R = 0.65$, whereas the later shows a shallow minimum at $R = 1.5$. We believe the first of these is likely the origin of the ubiquitous large peak in viscosity at around the surfactant to salt ratio $R = 0.65$. The general method of obtaining these free energies is transferrable to other surfactant solutions and can be used to compute their scission and branching free energies, which are the key ingredients that go into models for the dynamics and flow properties of micelles.

We are grateful for the financial support from the National Science Foundation under Grant No. CBET-0853662 and to the Procter and Gamble Company. Computational resources and services were provided in part by Advanced Research Computing at the University of Michigan, Ann Arbor, and in part through the Extreme Science and Engineering Discovery Environment (XSEDE, Grant No. TG-CHE140009).

*tmandal@umich.edu
†rlarson@umich.edu

[1] F. M. Menger and D. W. Doll, J. Am. Chem. Soc. **106**, 1109 (1984).
[2] D. Danino, Y. Talmon, H. Levy, G. Beinert, and R. Zana, Science **269**, 1420 (1995).
[3] F. Lequeux, Curr. Opin. Colloid Interface Sci. **1**, 341 (1996).
[4] S. Dhakal and R. Sureshkumar, J. Chem. Phys. **143**, 024905 (2015).
[5] J. Yang, Curr. Opin. Colloid Interface Sci. **7**, 276 (2002).
[6] G. C. Maitland, Curr. Opin. Colloid Interface Sci. **5**, 301 (2000).
[7] E. D. Burger, L. G. Chorn, and T. K. Perkins, J. Rheol. **24**, 603 (1980).
[8] S. Ezrahi, E. Tuval, and A. Aserin, Adv. Colloid Interface Sci. **128–130**, 77 (2006).
[9] M. E. Cates and S. J. Candau, J. Phys. Condens. Matter **2**, 6869 (1990).
[10] W. Carl, R. Makhloufi, and M. Kröger, J. Phys. II (France) **7**, 931 (1997).
[11] F. C. MacKintosh, S. A. Safran, and P. A. Pincus, J. Phys. Condens. Matter **2**, SA359 (1990).
[12] F. C. MacKintosh, S. A. Safran, and P. A. Pincus, Europhys. Lett. **12**, 697 (1990).
[13] R. Granek and M. E. Cates, J. Chem. Phys. **96**, 4758 (1992).
[14] R. Granek, Langmuir **10**, 1627 (1994).
[15] C. Oelschlaeger, M. Schopferer, F. Scheffold, and N. Willenbacher, Langmuir **25**, 716 (2009).
[16] C. Oelschlaeger, P. Suwita, and N. Willenbacher, Langmuir **26**, 7045 (2010).
[17] S. R. Raghavan and E. W. Kaler, Langmuir **17**, 300 (2001).
[18] W. Siriwatwechakul, T. LaFleur, R. K. Prud'homme, and P. Sullivan, Langmuir **20**, 8970 (2004).
[19] R. G. Larson, J. Rheol. **56**, 1363 (2012).
[20] W. Z. Zou and R. G. Larson, J. Rheol. **58**, 681 (2014).
[21] W. Z. Zou and R. G. Larson, Soft Matter **12**, 6757 (2016).
[22] W. Zou, X. Tang, M. Weaver, P. Koenig, and R. G. Larson, J. Rheol. **59**, 903 (2015).
[23] S. Dhakal and R. Sureshkumar, ACS Macro Lett. **5**, 108 (2016).
[24] A. V. Sangwai and R. Sureshkumar, Langmuir **27**, 6628 (2011).
[25] A. V. Sangwai and R. Sureshkumar, Langmuir **28**, 1127 (2012).
[26] X. Tang, P. H. Koenig, and R. G. Larson, J. Phys. Chem. B **118**, 3864 (2014).
[27] H. Wang, X. M. Tang, D. M. Eike, R. G. Larson, and P. H. Koenig, Langmuir **34**, 1564 (2018).
[28] S. J. Marrink, H. J. Risselada, S. Yefimov, D. P. Tieleman, and A. H. De Vries, J. Phys. Chem. B **111**, 7812 (2007).
[29] P. Wang, S. Pei, M. Wang, Y. Yan, X. Sun, and J. Zhang, J. Colloid Interface Sci. **494**, 47 (2017).
[30] A. Sambasivam, A. V. Sangwai, and R. Sureshkumar, Phys. Rev. Lett. **114**, 158302 (2015).
[31] See Supplemental Material at http://link.aps.org/supplemental/10.1103/PhysRevLett.121.038001 for details of the simulations, extra analysis, and figures and protocol for branching free energy calculations.
[32] S. Wang and R. G. Larson, Langmuir **31**, 1262 (2015).
[33] M. Parrinello and A. Rahman, J. Appl. Phys. **52**, 7182 (1981).
[34] G. Bussi, D. Donadio, and M. Parrinello, J. Chem. Phys. **126**, 014101 (2007).
[35] T. Odijk, J. Phys. Chem. **93**, 3888 (1989).
[36] R. Beringer, Phys. Rev. **131**, 1402 (1963).
[37] H. J. C. Berendsen, D. van der Spoel, and R. van Drunen, Comput. Phys. Commun. **91**, 43 (1995).

[38] G. A. Tribello, M. Bonomi, D. Branduardi, C. Camilloni, and G. Bussi, Comput. Phys. Commun. **185**, 604 (2014).
[39] M. E. Helgeson, T. K. Hodgdon, E. W. Kaler, and N. J. Wagner, J. Colloid Interface Sci. **349**, 1 (2010).
[40] L. J. Magid, Z. Han, G. G. Warr, M. A. Cassidy, P. D. Butler, and W. A. Hamilton, J. Phys. Chem. B **101**, 7919 (1997).
[41] Z. Wang and R. G. Larson, J. Phys. Chem. B **113**, 13697 (2009).
[42] T. M. Clausen, P. K. Vinson, J. R. Minter, H. T. Davis, Y. Talmon, and W. G. Miller, J. Phys. Chem. **96**, 474 (1992).
[43] L. J. Magid, Z. Han, Z. Li, and P. D. Butler, J. Phys. Chem. B **104**, 6717 (2000).
[44] P. A. Hassan, S. R. Raghavan, and E. W. Kaler, Langmuir **18**, 2543 (2002).
[45] F. Lequeux, Europhys. Lett. **19**, 675 (1992).
[46] M. In, G. G. Warr, and R. Zana, Phys. Rev. Lett. **83**, 2278 (1999).
[47] L. Ziserman, L. Abezgauz, O. Ramon, S. R. Raghavan, and D. Danino, Langmuir **25**, 10483 (2009).
[48] A. Khatory, F. Lequeux, F. Kern, and S. J. Candau, Langmuir **9**, 1456 (1993).